Core Plasma Design of the Compact Helical Reactor with a Consideration of the Equipartition Effect

T Goto, J Miyazawa, N Yanagi, H Tamura, T Tanaka, R Sakamoto, C Suzuki, R Seki, S Satake, M Nunami, M Yokoyama, A Sagara and the FFHR Design Group

National Institute for Fusion Science, Toki, Gifu, 502-5292 Japan

E-mail: goto.takuya@nifs.ac.jp

Abstract

Integrated physics analysis of plasma operation scenario of the compact helical reactor FFHR-c1 has been conducted. The DPE method, which predicts radial profiles in a reactor by direct extrapolation from the reference experimental data, has been extended to implement the equipartition effect. Close investigation of the plasma operation regime has been conducted and a candidate plasma operation point of FFHR-c1 has been identified within the parameter regime that has already been confirmed in LHD experiment in view of MHD equilibrium, MHD stability and neoclassical transport.

Keywords: heliotron, compact reactor design, plasma operation regime, equipartition effect, MHD stability, neoclassical transport

1. Introduction

Helical systems with net current-free plasma have an intrinsic advantage over a steady-state operation and are expected to be an alternative to tokamak systems as a fusion DEMO reactor and a commercial power plant. In the past six years, conceptual design activity of the helical fusion reactor FFHR-d1 has been conducted based on the achievement of the Large Helical Device (LHD) experiment [1]. This design activity has shown the design feasibility of a 1 GWe-class (with a 3 GW-class fusion output) commercial-scale power plant with the LHD-type heliotron configuration and the ITER-relevant technology. Integrated physics analysis of the core plasma performance of FFHR-d1 has been conducted with consideration of MHD equilibrium, MHD stability, neoclassical transport and boot-strap current. This analysis has shown that a fusion gain of $Q \sim 10$ is achievable within the physics parameter regime that has already been confirmed in the LHD experiment in the case of the high magnetic field option of FFHR-d1, called FFHR-d1B [2].

In the meantime, several innovative engineering design concepts have been proposed through the design activity. Among them, NITA coils [3], a pair of supplementary helical coils that have the minor radius of about 2 times that of main helical coils and have opposite-directed current of about −10%, provides a new prospect for the LHD-type helical reactor design. The NITA coils can enlarge the distance between the helical coils and the plasma, which is used as a space for the blanket modules, with almost no change in the plasma geometry. This enlargement indicates the design possibility of a smaller size reactor with keeping the blanket thickness. Recently, the target of a tokamak DEMO reactor has changed in both Japan and the EU. The target fusion output has been reduced to < 2 GW [4, 5]. In the EU roadmap of the Wendelstein stellarator line, an experimental machine called a burning stellarator has been proposed as an intermediate step before a stellarator commercial plant [6]. By considering such trends of the reactor design strategy, a new design option called FFHR-c1 has been proposed as an intermediate step to FFHR-d1. FFHR-c1 aims at a steady-state electric power generation over one year and satisfies the requirements on the Japanese DEMO reactor, i.e., electricity self-sufficiency, tritium self-sufficiency, and practical availability, with as small a reactor size as possible. According to the parametric scan by the systems code HELIOSCOPE [7], design point with the major radius of the helical coils $R_c = 10.92$ m and the magnetic field at the winding centre of the helical coils $B_c = 7.3$ T has been selected as a candidate of FFHR-c1. HELIOSCOPE predicts that a fusion gain of $Q > 10$ and positive

net electric output can be achieved at this design point. However, HELIOSCOPE adopts a quite simple gyro-Bohm-type scaling for the estimation of the energy confinement of the core plasma, i.e., the same plasma performance is assumed if the value of $R_c^4 B_c^3$ is kept. Therefore, the viability of $Q > 10$ achievement should be examined in more detail. In order to conduct a detailed physics analysis at a specified design point, information regarding radial profiles of plasma density and temperature are necessary. In this study, the model used for the prediction of radial profiles in the previous study was extended to deal with the equipartition effect. Using the modified model, integrated physics analysis of the possible operation regime of FFHR-c1 has been conducted by considering critical physics conditions: MHD equilibrium, MHD stability and neoclassical transport. Brief reviews of the calculation model and prerequisites of the calculation are given in Section 2. The results of calculation are given in Section 3. Finally, these are summarised in Section 4.

2. Calculation method

2.1. Implementation of equipartition effect to the direct profile extrapolation method

In order to predict radial profiles in a reactor, the method called Direct Profile Extrapolation (DPE) has been proposed [8]. In LHD experiment, gyro-Bohm type parameter dependence has been widely observed not only in global energy confinement but also in local relationship between the electron pressure and the electron density $p_e(\rho) \propto n_e(\rho)^{0.6}$ (ρ is normalised minor radius). This means that gyro-Bohm normalised pressure profile

$$\hat{p}(\rho) = \frac{p_{e,\mathrm{exp}}(\rho)}{P_{\mathrm{abs,exp}}^{0.4} B_{\mathrm{exp}}^{0.8}\, n_{e,\mathrm{exp}}(\rho)^{0.6}} \qquad (1)$$

is kept constant during a discharge. In Eq. (1), P_{abs} and B are the absorbed power and the magnetic field strength, respectively. The subscript 'exp' denotes that the parameters are obtained from the reference LHD experimental data. In the DPE method, the electron pressure profile of the reactor is estimated by using this normalised pressure profile

$$p_{e,\mathrm{reactor}}(\rho) = \gamma_{\mathrm{DPE}*} \hat{p}(\rho)\, P_{\mathrm{abs,reactor}}^{0.4} B_{\mathrm{reactor}}^{0.8}\, n_{e,\mathrm{reactor}}(\rho)^{0.6}, \qquad (2)$$

where the subscript 'reactor' denotes that the parameters are those of the reactor. $\gamma_{\mathrm{DPE}*}$ in Eq. (2) is the confinement improvement factor related to the peakedness of the heating profile [9]

$$\gamma_{\mathrm{DPE}*} = \left\{ \frac{\left(P_{\mathrm{dep}}/P_{\mathrm{dep1}}\right)_{\mathrm{avg,reactor}}}{\left(P_{\mathrm{dep}}/P_{\mathrm{dep1}}\right)_{\mathrm{avg,exp}}} \right\}^{0.6}, \qquad (3)$$

$$\left(P_{\mathrm{dep}}/P_{\mathrm{dep1}}\right)_{\mathrm{avg}} = \int_0^1 \frac{P_{\mathrm{dep}}(\rho)}{P_{\mathrm{dep}}(1)} \mathrm{d}\rho \quad , \qquad (4)$$

$$P_{\mathrm{dep}}(\rho) = \int_0^\rho P_{\mathrm{abs}}(\rho') \left(\frac{\mathrm{d}V}{\mathrm{d}\rho'}\right) \mathrm{d}\rho', \qquad (5)$$

where $P_{\mathrm{dep}}(\rho)$ is the deposition profile of the absorbed power.

In the previous study for FFHR-d1, temperature equality ($T_e = T_i$) was assumed and the total plasma pressure was assumed to be twice the electron pressure. However, alpha heating becomes predominant in the reactor condition with a high fusion gain. Regarding the auxiliary heating, electron cyclotron heating (ECH) is considered to be the most promising method for the following reasons: small influence on the blanket coverage because of its small port size, high core heating efficiency and capability of the protection of the device from fusion neutrons by using remote steering system. Therefore, electron heating will be dominant in any operation phase of FFHR-c1 and the temperature equality is not necessarily satisfied. To deal with such conditions with dominant electron heating, the DPE method has been modified as follows:

$$p_{e,\mathrm{reactor}}(\rho) = \gamma_{\mathrm{DPE}*,e} \hat{p}(\rho)\, P_{\mathrm{abs},e}^{0.4} B_{\mathrm{reactor}}^{0.8}\, n_{e,\mathrm{reactor}}(\rho)^{0.6}, \qquad (6)$$

$$p_{i,\mathrm{reactor}}(\rho) = \gamma_{\mathrm{DPE}*,i} \hat{p}(\rho)\, P_{\mathrm{abs},i}^{0.4} B_{\mathrm{reactor}}^{0.8}\, n_{i,\mathrm{reactor}}(\rho)^{0.6}, \qquad (7)$$

$$P_{\mathrm{abs},e} = \eta_\alpha P_\alpha + \eta_{\mathrm{aux},e} P_{\mathrm{aux},e} - P_{\mathrm{rad}} - P_{ei}, \quad (8)$$

$$P_{\mathrm{abs},i} = \eta_{\mathrm{aux},i} P_{\mathrm{aux},i} + P_{ei}, \quad (9)$$

where η_α $\eta_{\mathrm{aux},e}$ and $\eta_{\mathrm{aux},i}$ are absorption efficiency of the alpha heating power, auxiliary heating power to electrons and auxiliary heating power to ions, respectively.

The terms of the heating power and the power loss P_X ($X = \alpha$, aux, rad, ei) are calculated from the radial profiles $Q_X(\rho)$:

$$P_X = \int_0^1 Q_X(\rho) \frac{\mathrm{d}V}{\mathrm{d}\rho} \mathrm{d}\rho. \quad (10)$$

The equipartition power from electrons to ions is calculated by

$$Q_{ei}(\rho) = \frac{1.5 k_B \{T_e(\rho) - T_i(\rho)\} n_e(\rho)}{\tau_{ei}^{\varepsilon}(\rho)}, \quad (11)$$

where k_B and τ_{ei}^{ε} are Boltzmann constant and electron-ion energy relaxation time, respectively. To confirm the validity of the developed model, comparison with the experimental results has been carried out. The experimental data is from the NB heated hydrogen discharges ($P_{\mathrm{NBI}} \sim 4$ MW) superposed by ECH of ~ 4.8 MW with a different electron density (corresponds to the shots #126570, 126573, 126574 and 126576 at $t = 4.64$ s). In the calculation, the electron density profile and the normalised pressure profile were given as fitting functions of the experimental data. Confinement improvement factors $\gamma_{\mathrm{DPE}^*,e}$ and $\gamma_{\mathrm{DPE}^*,i}$ in Eqs. (6) and (7) were calculated from the profiles of NB heating power, EC heating power and equipartition power using Eq. (3). Regarding the NB heating profile, calculation results of FIT3D code [10] were used. Regarding the EC heating, perfect absorption of the injected power with the Gaussian profile that has a peak at the magnetic axis was assumed. The calculation results show a reasonable agreement with the experimental data as shown in Fig. 1.

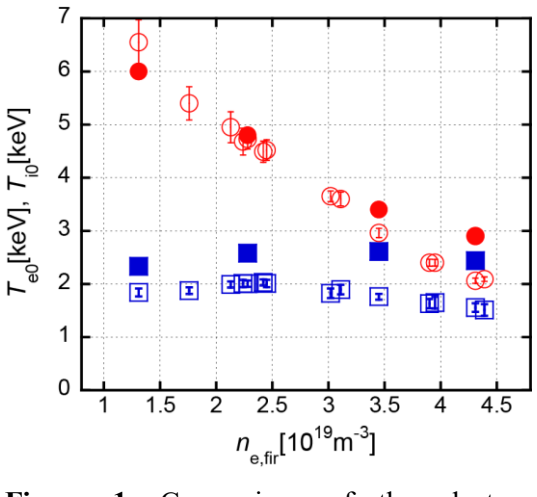

Figure 1. Comparison of the electron temperature (red circles) and ion temperature (blue squares) calculated by the developed model (closed symbols) with the LHD experimental data (open symbols).

2.2. Prerequisites of the calculation

In the design study of FFHR-d1, magnetic configuration with a high plasma aspect ratio with helical pitch parameter $\gamma_c = 1.2$ (where $\gamma_c = m a_c/(\ell R_c)$ and m, a_c and ℓ are toroidal pitch number ($m = 10$ in this case), helical coil minor radius and the number of helical coils ($\ell = 2$ in this case), respectively) and inward-shifted magnetic axis position (with the ratio between the magnetic axis position R_{ax} and R_c is 3.55/3.9) were selected for the following reasons. The first reason is that the space between the helical coil and the plasma increases with increasing the plasma aspect ratio. The second reason is the existence of the MHD equilibrium with a high beta. 3D equilibrium calculation by HINT2 code [11] has shown that MHD equilibrium with a similar shape of the flux surfaces to those in the vacuum condition can be

achieved by controlling the vertical field in the case of this configuration at the high beta up to $\beta_0 \sim 8\%$. In this study, the same magnetic configuration and the same reference experimental data as that in the previous study (#115787, t = 3.90 s) were selected. The gyro-Bohm normalised pressure profile of most of the LHD experimental data can be fitted by a single zero-order Bessel function

$$\hat{p}(\rho) = \alpha_0 J_0\left(\frac{2.4\rho}{\alpha_1}\right). \qquad (12)$$

In this case, α_0 = 1.42 and α_1 = 1.12. Using the normalised pressure profile, the relation between the electron temperature and the required amount of the auxiliary heating power is calculated with the following assumptions. Regarding the electron density, the very flat profile with a shoulder structure around ρ = 0.7 was assumed. This profile corresponds to that obtained by the calculation with the condition of no inward transport and particle source profile which is exactly the same as the ablation profile of the pellet calculated by the neural gas shielding (NGS) model [12]. Calculation with a typical reactor condition (e.g., $n_{e0} \sim 2\times10^{20}$ m^{-3}, T_{e0} ~ 10 keV, the size and injection velocity of the pellets are 5 mm and 1.5 km/s, respectively) gives the radial position of the ablation front around ρ = 0.7 as shown in Figs. 4 and 9 in Ref. [2]). Regarding the ion density profile, helium ash fraction of 5% is assumed and absolute value of the density of deuterons and tritons are given to be 0.45 times that of electrons at any radial position. No other impurity was considered in the calculation. The profiles used in the calculation are summarised in Fig. 2. Regarding the heating power, deposition profile of the alpha heating power is assumed to be the same as the alpha particle birth profile calculated from sthe radial profiles of the ion density and temperature. The absorption efficiency of the alpha heating power η_α = 85 % was assumed according to the result of alpha particle orbit calculation by MORH code for the high beta operation point of FFHR-d1 [8]. Assuming the use of ECH with the frequency adjusted to the magnetic field strength on the axis, the deposition profile of the auxiliary heating power to electrons is given as the Gaussian profile

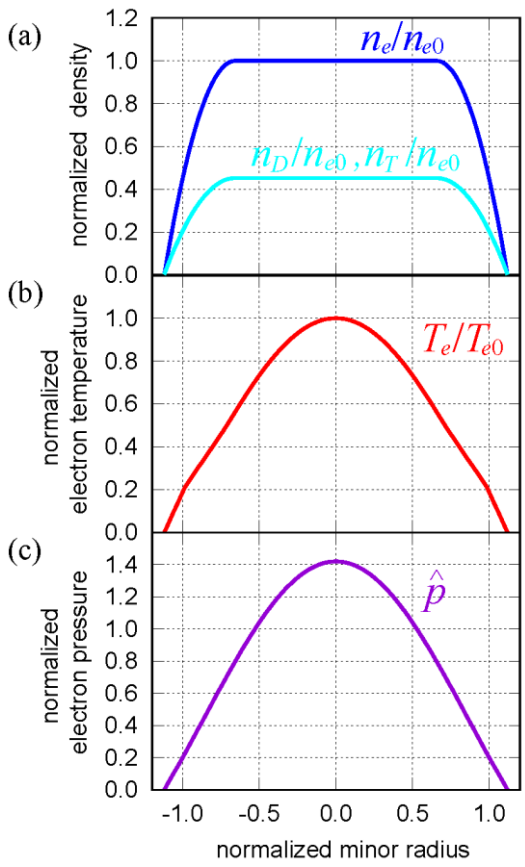

Figure 2. Radial profile of (a) the electron and ion density, (b) the electron temperature, and (c) the gyro-Bohm normalised pressure used in the calculation.

$$P_{\mathrm{aux},e}(\rho) = \frac{P_{\mathrm{ECH}}}{\sqrt{2\pi\sigma^2}}\exp\left(-\frac{\rho^2}{2\sigma^2}\right), \qquad (13)$$

with σ= 0.05 and no heating power to ions is considered ($P_{\mathrm{aux},i}$ =0). As described in the above, existence of the MHD equilibrium with a similar shape of the magnetic flux surfaces to those in the vacuum condition has been confirmed by HINT2 code. It has also found that VMEC [13] calculation with a fixed boundary shape that obtained from the HINT2 calculation gives a result consistent with that by HINT2 code. It means that the existence of MHD equilibrium is assured by VMEC calculation with a fixed boundary shape obtained from the HINT2 calculation. In the calculation of the radial profile of the heating power and the power loss, therefore, the volume of the flux surface at each radial position is obtained from the 3D equilibrium calculation by VMEC with a fixed boundary shape similar to that of high-beta equilibrium obtained in the previous study. Though ECH can generate anisotropic pressure and can affect the equilibrium [14], this effect is ignored in this study. As described in the next section, the central electron density and temperature considered as the operation regime of FFHR-d1 are ~2× 10^{20} m^{-3} and ~10 keV, respectively. The anisotropy will decrease at this parameter range. MHD stability

is evaluated by Mercier index D_I [15] and neoclassical transport is evaluated by GSRAKE [16] using the VMEC equilibrium.

3. Calculation result

Using the calculation model described in the previous section (Eqs. (3)–(13)), plasma operation regime of FFHR-c1 was examined. In the LHD experiment, plasma operation regime is limited mainly by MHD instability and energy confinement. For the former condition, it has been found that the operation regime of the LHD is limited when Mercier index D_I at low order rational surfaces exceeds a certain value. In the case of the magnetic configuration of this calculation (high plasma aspect ratio and inward-shifted magnetic axis position), rotational transform, $\iota/2\pi$, at plasma centre is larger than 0.5 and monotonically increases outward. Therefore, D_I at m/n = 1/1 rational surface (corresponding to the radial position with $\iota/2\pi$ = 1), which is a typical rational surface at the plasma edge, is of particular importance in this calculation. In high-beta discharges in the LHD experiment, it has been observed that a low-n MHD mode that causes core pressure collapse emerges when D_I at m/n = 1/1 rational surface exceeds 0.2–0.25, and this condition corresponds to the theoretical prediction [17, 18]. On the other hand, the growth rate of the instability decreases with increasing magnetic Reynolds number [19], which becomes larger in the reactor condition. Some experimental results indicate that the MHD stability is maintained with further larger value of the Mercier index. Thus, we selected D_I = 0.3 at m/n = 1/1 rational surface as an index of the MHD stability. For the latter condition, the estimated electron heat conduction coefficient corresponds to the 2-3 times of the prediction by the neoclassical theory according to the transport analysis of a typical LHD plasma [20]. Then we assume that the upper limit of the energy loss is estimated by neoclassical calculation with a deterioration factor of 2–3 here. In this study, the dependence of the operation regime on these critical physics parameters was analysed.

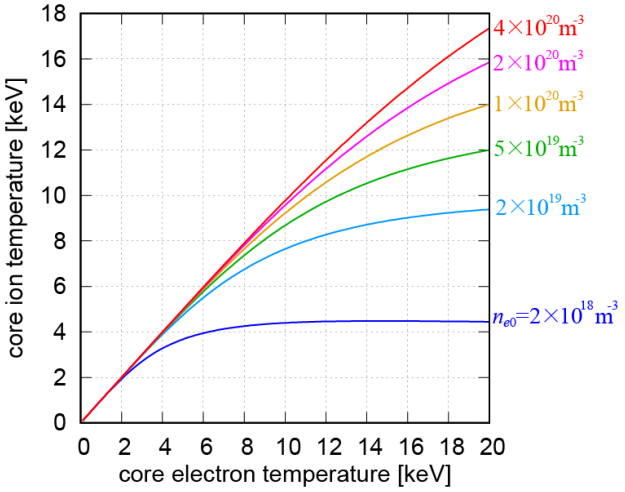

Figure 3. Core ion temperature of FFHR-c1 calculated by the developed model as a function of electron density and electron temperature.

Figure 3 shows the calculated ion temperature as a function of electron density and temperature. Though the difference between electron temperature and ion temperature becomes large in the region with low density and high temperature, temperature equality is almost satisfied within the region considered as a reactor condition: $n_{e0} \sim 2\times10^{20}\,\mathrm{m}^{-3}$, $T_{e0} \sim 10\,\mathrm{keV}$. On the other hand, the required power to sustain the plasma with the same electron density and electron temperature becomes large compared with the case in which temperature equality is assumed, as shown in Fig. 4. Because no direct heating power to ions is considered ($P_{\mathrm{aux},i}$ = 0), total absorbed power to ions is equal to the equipartition power ($P_{\mathrm{abs},i} = P_{ei}$). That is because the heating profile of ions by equipartition power has a broader profile compared with alpha heating

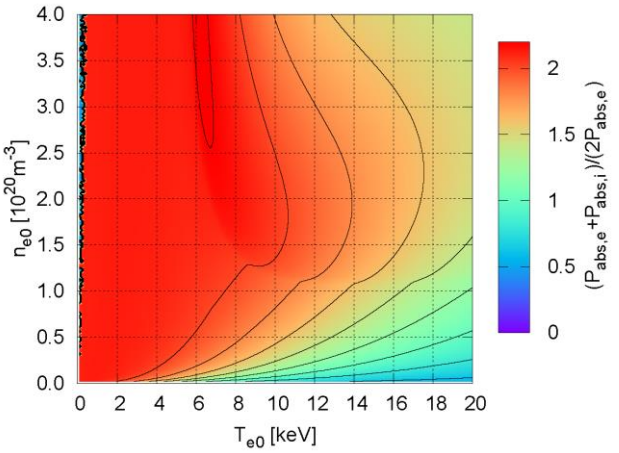

Figure 4. The ratio of the required power calculated by Eqs. (3)–(13) to the required power calculated with the assumption of temperature equality.

and auxiliary heating. As described by Eqs. (3)–(5), broader heating profile leads to smaller confinement improvement factor of ions, $\gamma_{DPE^*,i}$, resulting in the requirement of larger power to sustain the plasma with the same central ion temperature. Figure 5 shows the plasma operation contour (POPCON) plot. The contours of Mercier index D_I at $m/n = 1$ rational surface, the maximum value in the radial profile of the ratio of the neoclassical transport loss to the volume integrated absorbed power $(Q_{neo}S/P_{abs})_{max}$ (P_{abs} is the total absorbed power, i.e., the sum of alpha heating power and auxiliary heating power subtracted by Bremsstrahlung loss), the peak beta value, the fusion power and the fusion gain are plotted. If the operation regime is limited by the condition of $D_I < 0.3$ and $(Q_{neo}S/P_{abs})_{max} < 0.5$ (corresponds to the condition that the energy loss is twice that predicted by neoclassical theory), fusion gain of $Q = 10$ can be achieved in FFHR-c1 with $n_{e0} \sim 2.3 \times 10^{20}$ m^{-3} and $T_{e0} \sim 11.5$ keV. On the other hand, it has been observed that the achievable peak beta value β_0 is limited due to the core pressure collapse especially in the condition with inward-shifted magnetic axis position. In this operation point with $Q = 10$, the calculated magnetic axis position is $R_{ax}/R_c \sim 3.67/3.9$. In the LHD experiment, β_0 is limited up to ~2.5% at this magnetic axis position [21]. This upper limit of the peak beta value is quite sensitive to the magnetic axis position. The magnetic axis position depends on the magnetic configuration (i.e., winding law of helical coils and current of poloidal coils in the case of the LHD-type heliotron devices). Therefore, a slight change in the winding law of helical coils or current of poloidal coils might provide a solution.

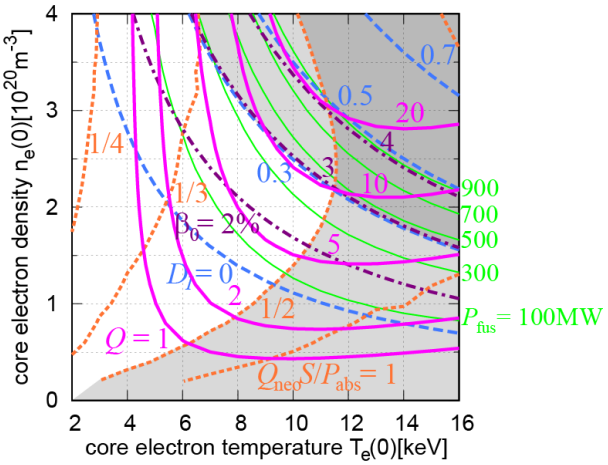

Figure 5. POPCON plot at the steady-state operation point of FFHR-c1. Contours of the fusion power (thin solid green curve), the fusion gain (thick solid magenta curve), the peak beta value (dashed-dotted maroon curve), the Mercier index (broken blue curve) and the ratio of the neoclassical energy loss to the total absorbed power (dotted orange curve) are plotted. The region without shading corresponds to the operation regime with the physics conditions that have already been confirmed by the LHD experiment.

4. Summary

Integrated physics analysis of the plasma operation regime for an LHD-type compact helical fusion reactor FFHR-c1 was examined by detailed physics analysis tools with consideration of the equipartition effect. It has been shown that steady-state operation with a fusion gain of $Q \sim 10$ can be achieved within a plasma operation regime that is consistent with the LHD experiment in view of MHD equilibrium, MHD stability, neoclassical transport and alpha energy loss. The modified model also enables a quantitative analysis of the operation regime with various reference profiles and magnetic configurations. Although additional quantitative analysis of anomalous transport and boot-strap current as well as optimum selection of the magnetic configuration is required, this study shows the design feasibility of a compact LHD-type helical reactor as an intermediate step to the LHD-type helical commercial power plants.

Acknowledgments

This work is supported by the budget NIFS10ULFF011 of National Institute for Fusion Science and MEXT/JSPS KAKENHI Grant Number 24760704. The authors also appreciate the members of the Fusion Engineering Research Project, the LHD project and the Numerical Simulation Reactor Research Project in NIFS for providing valuable comments and advice.

References

[1] Sagara A. *et al* 2017 *Nucl. Fusion* **57** 086046
[2] Goto T. *et al* 2017 *Nucl. Fusion* **57** 066011
[3] Yanagi N. *et al* 2016 *Plasma Fusion Res.* **11** 2405034
[4] Sakamoto Y. *et al* 2014 *Fusion Eng. Des.* **89** 2440
[5] Federici G. *et al* 2014 *Fusion Eng. Des.* **89** 882
[6] Warmer F. *et al* 2016 *Plasma Phys. Control. Fusion* **58** 074006
[7] Goto T. *et al* 2011 *Nucl. Fusion* **51** 083045
[8] Miyazawa J. *et al* 2014 *Nucl. Fusion* **54** 043010
[9] Miyazawa J. *et al* 2014 *Nucl. Fusion* **54** 013014
[10] Vincenzi P. *et al* 2016 *Plasma Phys. Control. Fusion* **58** 125008
[11] Suzuki Y. *et al* 2006 *Nucl. Fusion* **46** L19
[12] Parks P.B. *et al* 1978 *Phys. Fluids* **21** 1735
[13] Hirshman S.P. *et al* 1983 *Phys. Fluids* **26** 3553
[14] Asahi Y. *et al* 2011 *Plasma Fusion Res.* **6** 2403123
[15] Glasser A. H. *et al* 1975 *Phys. Fluids* **18** 875
[16] Beidler C.D. *et al* 1995 *Plasma Phys. Control. Fusion* **37** 463
[17] Yamada H. *et al* 2004 *J. Plasma Fusion Res. SERIES* **6** 51
[18] Sakakibara S. *et al* 2006 *Proc. of 21st IAEA Fusion Energy Conf. (Chengdu, China, 2006)* EX/7-5
[19] Sakakibara S. *et al* 2008 *Plasma Phys. Control. Fusion* **50** 124014
[20] Yamada H. *et al* 2010 *Phys. Rev. Lett.* **84** 1216
[21] Komori A. *el al* 2009 *Nucl. Fusion* **49** 104015